Electrochemistry of $[MoS_2(C_5H_{10}NO)_2]$ and Its Oxo–Thio and Dioxo Analogs: Redox-Induced Interconversion of Species

Peter R. Traill,[1a] Alan M. Bond,* and Anthony G. Wedd*,[1b]

Department of Chemistry, La Trobe University, Bundoora, Victoria 3083, Australia

Received June 4, 1993[⊗]

Electrochemical reduction of the piperidine *N*-oxido complexes $MoS_2(C_5H_{10}NO)_2$, $MoOS(C_5H_{10}NO)_2$ and $MoO_2(C_5H_{10}NO)_2$ has been studied in detail by cyclic voltammetry, hydrodynamic voltammetry, and bulk electrolysis in aprotic organic solvents. Depending on the time domain, temperature or compound, a reversible one-electron reduction process or an overall irreversible process involving the apparent transfer of between 1 and 2 electrons may be observed. The initial reversible electron transfer process is metal-based and produces a transient molybdenum(V) complex $[Mo^{V}XY(C_5H_{10}NO)_2]^-$ (X and Y = O or S) which may be detected voltammetrically in the case of $[MoS_2(C_5H_{10}NO)_2]^-$ and $[MoOS(C_5H_{10}NO)_2]^-$. By contrast, on longer time domains, the overall irreversible process generates the reduced form of the ligand, $C_5H_{10}NH$, as well as free ligand itself, $C_5H_{10}NOH$, and involves redox-induced interconversion of the metal complexes. For example, $MoS_2(C_5H_{10}NO)_2$ is converted to $MoOS(C_5H_{10}NO)_2$ and $MoO_2(C_5H_{10}NO)_2$ with the oxo complexes being identified on the voltammetric time scale as well as by ^{95}Mo NMR measurements on the much longer synthetic time scale. The mechanism for the redox interconversion is complex, but is probably associated with an internal redox reaction where piperidine *N*-oxido ligand appears to act as an oxygen atom transfer reagent.

Introduction

The redox properties of $[Mo^{VI}O_2]^{2+}$ centers have been studied in detail because of their role in the catalytic properties of certain enzymes and industrial catalysts.[2-4] Oxidation states VI, V, and IV are involved in these catalytic reactions, and the way in which the properties are modulated by sulfur ligands is believed to be crucial. Sulfur ligation appears to be essential for enzyme activity[4] and also affects activity in heterogeneous industrial catalysis. Both acid–base and redox properties are altered significantly by oxo–thio exchange.[3-6] Substitution of sulfur for oxygen makes $[Mo^{VI}X_2]^{2+}$ (X = O or S) centers easier to reduce, and the redox processes become more reversible.[7,8]

Complexes containing the *cis* centers $[Mo^{VI}O_2]^{2+}$, $[MoOS]^{2+}$ and $[MoS_2]^{2+}$ bound to N,N-dialkylhydroxylamido ligands have been examined intensively.[9-14] For the piperidine *N*-oxido complexes $MoXY(C_5H_{10}NO)_2$ (XY = OO, OS, SS), Bristow et al.[13] have noted reduction peak potentials in dimethylformamide at, respectively, −1.59, −1.94, and −2.50 V vs SCE. Evidence is provided that the XY = OS and SS species show chemically reversible behavior at low temperatures. However, truncation of the room temperature voltammograms after the initial reduction step in each case masked an interesting interrelationship which is examined in the present work. An earlier contribution from these laboratories[14] explored the reaction of $MoOS(C_5H_{10}NO)_2$ with cyanide in the context of the inactivation of molybdenum enzymes by cyanide. It was shown that $MoOS(C_5H_{10}NO)_2$ reacts to produce $MoO_2(C_5H_{10}NO)_2$ and thiocyanate. Since free $C_5H_{10}NH$ and $C_5H_{10}NOH$ are also formed, the result suggested that the piperidine *N*-oxido ligand acts as the source of oxidising equivalents and that an internal redox reaction may occur during the course of the reaction. $MoS_2(C_5H_{10}NO)_2$ and $MoOSe(C_5H_{10}NO)_2$ also react with cyanide under the same conditions to form $MoO_2(C_5H_{10}NO)_2$, which suggests that internal redox reactions and the ligand exchange processes may be related. A systematic study of the voltammetric reduction of the $MoXY(C_5H_{10}NO)_2$ complexes was undertaken to probe the possible relationships.

Experimental Section

Abbreviations and parameter symbols are given in ref 15.

Synthesis and Sampling. The compounds $MoXY(C_5H_{10}NO)_2$ (XY = OO, OS,SS) were prepared and purified by the methods of refs 14 and 16.

Solvents and solutions were handled using standard Schlenck techniques. High purity dinitrogen was further purified by passage

⊗ Abstract published in *Advance ACS Abstracts,* October 1, 1994.

(1) (a) Present address: Department of Chemistry, University of Tasmania, Hobart, Tasmania, 7000, Australia. (b) Present address: School of Chemistry, University of Melbourne, Parkville, Victoria 3052, Australia.
(2) Mitchell, P. C. H. In *Proceedings of the Fourth International Conference on the Chemistry and Uses of Molybdenum*; Eds. Barry, H. P., Mitchell, P. C. H., Eds.; Climax Molybdenum Co.: Ann Arbor, MI, 1982; p 336.
(3) (a) Stiefel, E. I. *Prog. Inorg. Chem.* **1977**, *22*, 1. (b) Spence, J. T. *Coord. Chem. Rev.* **1983**, *48*, 59. (c) Spivack, B.; Dori, Z. *Coord. Chem. Rev.* **1975**, *17*, 99.
(4) (a) Holm, R. H. *Coord. Chem. Rev.* **1990**, *100*, 183. (b) Young, C. G.; Wedd, A. G. In *Molybdenum Enzymes, Catalysts and Models*; Coucouvanis, D., Newton, W. E., Stiefel, E. I., Eds.; American Chemical Society: Washington, DC, 1993; p 70.
(5) Holm, R. H. *Chem. Rev.* **1987**, *87*, 1401.
(6) Caradonna, J. P.; Reddy, P. R.; Holm, R. H. *J. Am. Chem. Soc.* **1988**, *110*, 2139.
(7) Taylor, R. D.; Street, F. P.; Minelli, M.; Spence, J. T. *Inorg. Chem.* **1978**, *17*, 3207.
(8) (a) You, J.; Wu, D.; Liu, H. *Polyhedron* **1986**, *5*, 535. (b) Kony, M. Ph.D. Thesis, La Trobe University, 1988. (c) Pratt, D. E.; Laurie, S. H.; Dahm, R. H. *Inorg. Chim. Acta* **1987**, *132*, L21. (d) Miller, K. F.; Bruce, A. E.; Corbin, J. L.; Wherland, S.; Stiefel, E. I. *J. Am. Chem. Soc.* **1980**, *102*, 5102 and references therein.
(9) Hofer, E.; Holzbach, W.; Wieghardt, K. *Angew. Chem., Int. Ed. Engl.* **1981**, *20*, 282.
(10) Wieghardt, K.; Hahn, M.; Weiss, J.; Swiridoff, W. *Z. Anorg. Allg. Chem.* **1982**, *492*, 164.
(11) Bristow, S.; Collison, D.; Garner, C. D.; Clegg, W. *J. Chem. Soc., Dalton Trans.* **1983**, 2495.
(12) Minelli, M.; Enemark, J. H.; Wieghardt, K.; Hahn, M. *Inorg. Chem.* **1983**, *22*, 3952.
(13) Bristow, S.; Garner, C. D.; Pickett, C. J. *J. Chem. Soc. Dalton Trans.* **1984**, 1617.
(14) Traill, P. R.; Tiekink, E. R. T.; O'Connor, M. J.; Snow, M. R.; Wedd, A. G. *Aust. J. Chem.* **1986**, *39*, 1287.

0020-1669/94/1333-5754$04.50/0

through three 3 Å molecular sieve towers and three R3-11 BASF catalyst towers for removal of H_2O and O_2, respectively. Solvents were purified as follows: (a) Dimethylformamide, DMF, (BDH, AnalR) was predried by stirring it over CaH_2 for 16 h and then over BaO for 16 h. It was sequentially dried three times by 3 Å molecular sieves over a period of 96 h and then twice fractionally distilled from clean sodium and anthracene under nitrogen at reduced pressure (1−2 mmHg) using a darkened distillation apparatus. The middle 70% fraction was collected and stored under nitrogen in the dark for no longer than 7 days before use.[17] (b) Tetrahydrofuran, THF, (May and Baker, Pronalys AR) was stirred with ferrous sulfate for 24 h and then predried with CaH_2. It was twice distilled under nitrogen from clean sodium and benzophenone, the central 80% fraction collected and stored under nitrogen in the dark.[18,19] (c) Acetonitrile, MeCN, (May and Baker, Laboratory Chemical) was predried with CaH_2 and then 4 Å molecular sieves. It was distilled off P_2O_5 under nitrogen, with the middle 80% fraction collected and stored under nitrogen in the dark. (d) Dichloromethane, CH_2Cl_2, (ICI, Laboratory Grade) was washed with concentrated H_2SO_4 (5 times), water, 5% aqueous NaOH, and water again, and then predried over anhydrous $CaCl_2$. It was distilled under nitrogen from CaH_2 and the middle 80% fraction collected and stored under N_2 in the dark.[18,20]

Solutions used in the glovebox (<1 ppm H_2O, <1 ppm O_2) were made up externally and transferred into the glovebox via the vacuum port. The cells were linked to the external control and voltammetric instrumentation via a wiring breakthrough incorporated into the glovebox. Solutions in the glovebox were maintained in a closed cell and were purged and blanketed by passing purified argon.

Electrochemistry. Unless otherwise specified, solutions contained 0.2 M $Bu^n_4NBF_4$ (Southwestern Analytical) as the electrolyte which was dried at 150 °C under vacuum prior to use.

A BAS CV-27 Voltammograph coupled with a Bausch and Lomb Houston Series 100 X-Y recorder was used for all voltammetric measurements. The electrochemical cell was a Princeton Applied Research design (10 cm^3 volume) incorporating the relevant electrodes. The temperature was monitored internally via a thermocouple and controlled by immersing the cell in either a thermostated water bath or an appropriate organic solvent slush bath. The cells were stored in an oven (110 °C) prior to use and were purged with purified nitrogen for 30 min prior to solution addition.

Platinum and glassy-carbon disk working electrodes used in cyclic voltammetry were Metrohm Type 2-628 and were polished with alumina prior to each experiment. The response on multiple scans of the sulfur-containing species was not reproducible due to electrode fouling. Consequently only data obtained on first scans are reported and the electrode was polished between each scan. The auxiliary electrode was platinum gauze (area 1.4 cm^2) while the reference electrode was an acetonitrile $Ag/AgNO_3$ (0.1 M) electrode incorporated into a salt bridge containing the solvent (supporting electrolyte) of interest to minimize contamination of the sample solution. The reference electrode was calibrated repeatedly against the Fc^+/Fc couple in both the external and internal modes.[21] Solutions were examined at three concentrations of $MoXY(C_5H_{10}NO)_2$ (2.0, 0.5, and 0.20 mM).

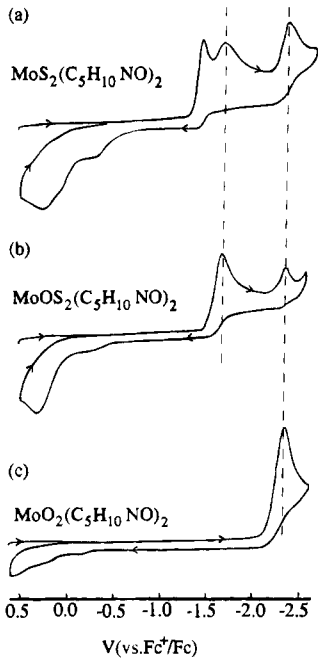

Figure 1. Cyclic voltammograms (v, 300 mV s^{-1}; 25 °C) of 2 mM solutions in DMF (0.2 M $Bu^n_4NBF_4$) at a glassy carbon electrode.

The Fc^+/Fc couple is known to satisfy the criteria for an electrochemically reversible, diffusion-controlled one electron charge-transfer process (cyclic voltammetry: ΔE_p = 56 mV at 25 °C: $i_p v^{-1/2}$ independent of v). Due to uncompensated (ohmic) *IR* drop and a time lag in the recorder, a range of values was observed for 0.2−2 mM solutions in DMF: ΔE_p = 60−88 mV and $i_p v^{-1/2}$ = 24−29 mA cm^{-2} M^{-1} $mV^{-1/2}$ $s^{1/2}$ (v = 20−1000 mV s^{-1}). Analogous behavior for redox couples studies in this work was taken as evidence for electrochemical reversibility.

Rotating disk voltammetry employed a Metrohm Model 628.10 drive unit and Metrohm electrodes. For Fc^+/Fc, the limiting current, i_L, was proportional to both $\omega^{1/2}$ and concentration as expected when the magnitude of i_L is mass-transfer-controlled. Furthermore, a plot of E against ln $[(i_L - i)/i]$ for ferrocene was linear with slope close to the Nernstian value of RT/F and had an intercept equal to $E^f_{1/2}$. These data suggested that the theoretical response could be obtained directly with rotating disk voltammetry.

For controlled-potential electrolysis experiments, a Bioanalytical Systems SP-2 synthetic potentiostat coupled to a Toshnin Electron TO2N1 copy recorder was used. The working electrode was a cylindrical platinum gauze (area approximately 22.6 cm^2) and the auxiliary electrode a platinum gauze strip enclosed in a salt bridge containing solvent and electrolyte.

Physical Measurements. ^1H, ^{13}C, and ^{95}Mo NMR spectra for species generated by bulk electrolysis were obtained on a JEOL FX-200 spectrometer. ESR data on the products of electrolysis were obtained with a Varian E-9 spectrometer. *In situ* electrochemical reduction of $MoS_2(C_5H_{10}NO)_2$ was undertaken at a platinum working electrode in the cavity of the ESR instrument using the ESR−electrochemical cell described in ref 22.

Results and Discussion

Initial Observations. Cyclic voltammograms of samples of $MoXY(C_5H_{10}NO)_2$ (XY = SS, OS, OO) confirmed as *spectroscopically pure* by ^1H, ^{13}C, and ^{95}Mo NMR are shown in Figure 1. DMF was the solvent of choice for most of the voltammetric studies as other solvents tested either did not have a sufficiently negative potential range available to observe reduction of $MoO_2(C_5H_{10}NO)_2$ or else appeared to react with the products of the reduction process. The order of reduction potentials of

(15) *Abbreviations*: E, potential; i, current; Fc^+/Fc, ferrocenium/ferrocene; $E^f_{1/2}$, reversible half-wave potential; E_p, peak potential; ΔE_p, peak-to-peak separation; v, scan rate; i_L, limiting current; i_p, peak current; i_p^{red}, reduction peak current; i_p^{ox}, oxidation peak current; ω, electrode rotation frequency; n, number of electrons per molecule transferred in the charge transfer process; n_{app}, the apparent value of n.

(16) McDonell, A. C.; Vasudevan, S. G.; O'Connor, M. J.; Wedd, A. G. *Aust. J. Chem.* **1985**, *38*, 1017.
(17) (a) Burfield, D. R.; Smithers, R. H. *J. Org. Chem.* **1978**, *43*, 3966. (b) Clack, D. W.; Hush, N. S. *J. Am. Chem. Soc.* **1965**, *87*, 4238. (c) Juillard, J. *Pure Appl. Chem.* **1977**, *49*, 885. (d) Moe, N. S. *Acta Chem. Scand.* **1967**, *21*, 1389.
(18) Perrin, D. D.; Armarego, W. L. F.; Perrin, D. R. *Purification of Laboratory Chemicals*, 2nd ed.; Pergamon Press: Oxford, England, 1980.
(19) (a) Coetzee, J. F.; Chang, T. H. *Pure Appl. Chem.* **1985**, *57*, 633. (b) Burfield, D. R.; Lee, K. H.; Smithers, R. H. *J. Org. Chem.* **1977**, *42*, 3060. (c) Burfield, D. R. *J. Org. Chem.* **1984**, *49*, 3852.
(20) Kadish, K. M.; Anderson, J. E. *Pure Appl. Chem.* **1987**, *59*, 703.
(21) Gagné, R. R.; Koval, C. A.; Lisensky, G. C. *Inorg. Chem.* **1980**, *19*, 2854 and references therein.
(22) Bagchi, R. N.; Bond, A. M.; Colton, R. *J. Electroanal. Chem.* **1986**, *199*, 297.

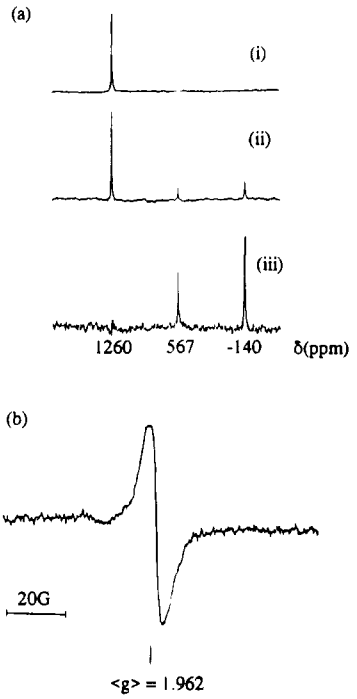

Figure 2. Spectroscopic monitoring of the electrolytic reduction of a 20 mM solution of $MoS_2(C_5H_{10}NO)_2$ at a platinum electrode at 25 °C: (a) ^{95}Mo NMR spectra in MeCN (0.2 M $Bu^n_4NBF_4$), with (i) initial spectrum, (ii) spectrum obtained after 2 h, and (iii) spectrum after exhaustive electrolysis (12 h); (b) ESR spectrum in CH_2Cl_2 (0.1 M $Bu^n_4NBF_6$).

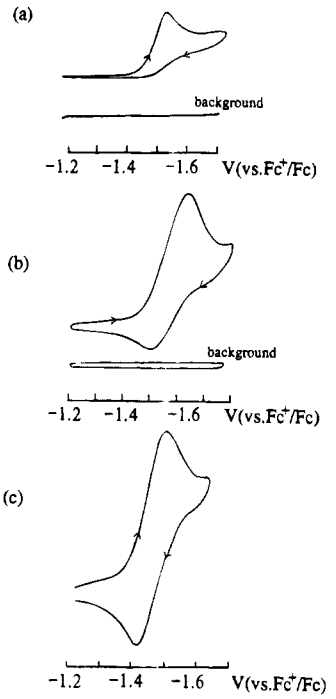

Figure 3. Cyclic voltammograms of $MoS_2(C_5H_{10}NO)_2$ (2 mM solutions in DMF (0.2 M $Bu^n_4NBF_4$)) at a glassy carbon electrode: (a) $\nu = 100$ mV s^{-1}, 25 °C; (b) $\nu = 500$ mV s^{-1}, 25 °C; (c) $\nu = 500$ mV s^{-1}, −60 °C.

the first process is SS < OS < OO, confirming the previous work.[13] However, reduction of $MoS_2(C_5H_{10}NO)_2$ clearly gives two additional reduction processes at more negative potentials and oxidation processes are observed on the reverse scan of the cyclic voltammogram. The additional processes are not described in ref 13. Interestingly, the two more negative reduction processes correspond to production and subsequent reduction of the OS and OO species by comparison of the peak potentials with those obtained using authentic samples (as indicated in Figure 1). Additionally, reduction of $MoOS(C_5H_{10}NO)_2$ provides a second reduction process which corresponds to formation and subsequent reduction of the OO compound. In each case, oxidation processes on the reverse scans are observed at around 0 V vs Fc^+/Fc in the cyclic voltammograms, indicating that processes other than oxygen-sulfur exchange occur. Previous work[13] did not address any of these features, presumably because the voltammograms were truncated after the initial reduction step.

Identification of both $MoOS(C_5H_{10}NO)_2$ and $MoO_2(C_5H_{10}NO)_2$ as products of the reduction of $MoS_2(C_5H_{10}NO)_2$ were confirmed by controlled-potential reductive electrolysis of $MoS_2(C_5H_{10}NO)_2$ in acetonitrile (0.2 M $Bu^n_4NBF_4$) at −1.6 V vs Fc^+/Fc. Monitoring the course of the process by ^{95}Mo NMR spectroscopy (Figure 2a) revealed new peaks at 567 and −140 ppm (OS and OO species respectively) increasing in intensity at the expense of the peak at 1260 ppm (SS species). ^{95}Mo NMR chemical shifts are 0−40 ppm less positive in acetonitrile (electrolyte) compared to those reported previously in $CDCl_3$.[14] *In situ* controlled-potential electrolysis experiments in the cavity of an ESR spectrometer in CH_2Cl_2 (0.1 M $Bu^n_4NPF_6$) led to the observation of the spectrum shown in Figure 2b. The signal disappeared immediately upon interruption of the electrolysis, suggesting the presence of a Mo^V intermediate. The g value of 1.96 is typical of sulfur-containing Mo^V species.[4]

$MoS_2(C_5H_{10}NO)_2$: The Charge Transfer Step. The observation of an overall redox process involving interconversion of sulfur to oxygen ligands implies that a chemical reaction(s) is coupled to the charge transfer process. Cyclic voltammetric experiments demonstrate that the first reductive response is irreversible at 25 °C and $\nu = 10$ mV s^{-1} but becomes chemically reversible at −60 °C and $\nu \geq 100$ mV s^{-1} (Figure 3). Analysis of data at 25 °C (Table 1) suggests that chemical steps follow the initial charge transfer. Figure 3 shows that they can be outrun at low temperature and/or fast scan rates.

Provided that the chemical reactions following the charge transfer steps are sufficiently slow relative to the electrode rotation rate, hydrodynamic voltammetry at a rotating disk electrode (Figure 4) allows some details of the electron transfer step to be studied more readily than via cyclic voltammetry.[23] Where a relatively fast DC scan rate of 100 mV s^{-1} is employed, this scan rate combined with high rotation rates minimizes the influence of any adsorption or other reactions following the charge transfer process. With the DC scan rate of 100 mV s^{-1} a plot of the limiting current, i_L, versus $\omega^{1/2}$ is linear with a zero intercept at high rotation rates (Figure 4b), i_L also is a linear function concentration (Figure 4c) while plots of E versus $\ln[(i_L - i)/i]$ (Figure 4d) are linear with a slope of (26 ± 1) mV and independent of concentration for rotation rates ≥157 rad s^{-1}. The intercepts and slopes of plots of E versus $\ln[(i_L - i)/i]$ provide an estimate of the reversible half-wave potential, $E^r_{1/2} = -1.45 \pm 0.01$ V vs Fc^+/Fc and of $n = 1.0$ electron per molecule assuming that the electron transfer process is reversible. Additionally, the second and third reduction processes are almost absent at the rotating disk electrode when fast rotation rates are used so the assumption that the chemical steps following the charge transfer are not greatly influencing the hydrodynamic voltammetric experiments seems to be valid. Data obtained at the rotating disk electrode at high rotation rates are therefore consistent with an essentially chemically and electrochemically reversible diffusion-controlled redox couple:

(23) Bard, A. J., Faulkner, L. R., Eds. *Electrochemical Methods*; Wiley: New York, 1980; Chapter 8.

Table 1. Cyclic Voltammetric Data for $MoS_2(C_5H_{10}NO)_2$ in DMF (0.2 M $Bu^n_4NBF_4$) at a Glassy-Carbon Electrode[a] with Data for Oxidation of Ferrocene Given in Parentheses

concn	ν	E_p^{red} [b]	ΔE_p	i_p^{red}	$i_p^{red}\nu^{-1/2}$	i_p^{ox}/i_p^{red}
2.00 (25 °C)	20	−1.52 (0.07)	... (61)	68.3 (109.2)	15.3 (24.4)	... (1.1)
	50	−1.53 (0.07)	... (60)	108.5 (179.6)	15.3 (25.4)	... (1.0)
	100	−1.53 (0.07)	... (57)	157.7 (260.6)	15.8 (26.1)	... (1.0)
	300	−1.53 (0.06)	84 (71)	266.2 (458.4)	15.4 (26.5)	0.4 (1.0)
	500	−1.54 (0.06)	84 (79)	327.5 (584.5)	14.6 (26.1)	0.4 (1.0)
	800	−1.54 (0.06)	89 (82)	374.6 (697.5)	13.3 (24.6)	0.6 (1.0)
	1000	−1.54 (0.06)	91 (86)	395.8 (750.7)	12.5 (23.7)	0.7 (1.0)
0.50 (25 °C)	20	−1.52 (0.07)	... (64)	78.9 (123.2)	17.6 (27.6)	... (1.0)
	50	−1.53 (0.07)	... (65)	125.6 (152.8)	17.8 (21.6)	... (1.0)
	100	−1.53 (0.07)	... (64)	181.4 (276.1)	18.1 (27.6)	... (1.0)
	300	−1.53 (0.07)	81 (70)	309.9 (466.9)	17.9 (27.0)	0.4 (1.0)
	500	−1.54 (0.07)	83 (73)	379.2 (586.6)	17.0 (26.2)	0.4 (1.0)
	800	−1.54 (0.06)	90 (82)	430.4 (687.3)	15.2 (24.3)	0.6 (1.0)
	1000	−1.54 (0.06)	95 (88)	451.8 (729.6)	14.3 (23.1)	0.7 (1.0)
2.00 (55 °C)	20	−1.52		131.7	29.5	
	50	−1.51		186.6	26.4	
	100	−1.52		256.3	25.6	
	300	−1.55		403.5	23.3	
	500	−1.56		500.0	22.4	
	800	−1.59		553.5	19.6	

[a] Units: concn mM; ν, mV s^{-1}; E_p^{red}, V; $\Delta E_p = (E_p^{ox} - E_p^{red})$, mV; i_p^{red}, mA cm^{-2} M^{-1}; $i_p^{red}\nu^{-1/2}$, mA cm^{-2} M^{-1} $mV^{-1/2}$ $s^{1/2}$. [b] V vs Fc^+/Fc for $MoS_2(C_5H_{10}NO)_2$ data and V vs Ag/Ag^+ (0.1 M $AgNO_3$) for ferrocene data.

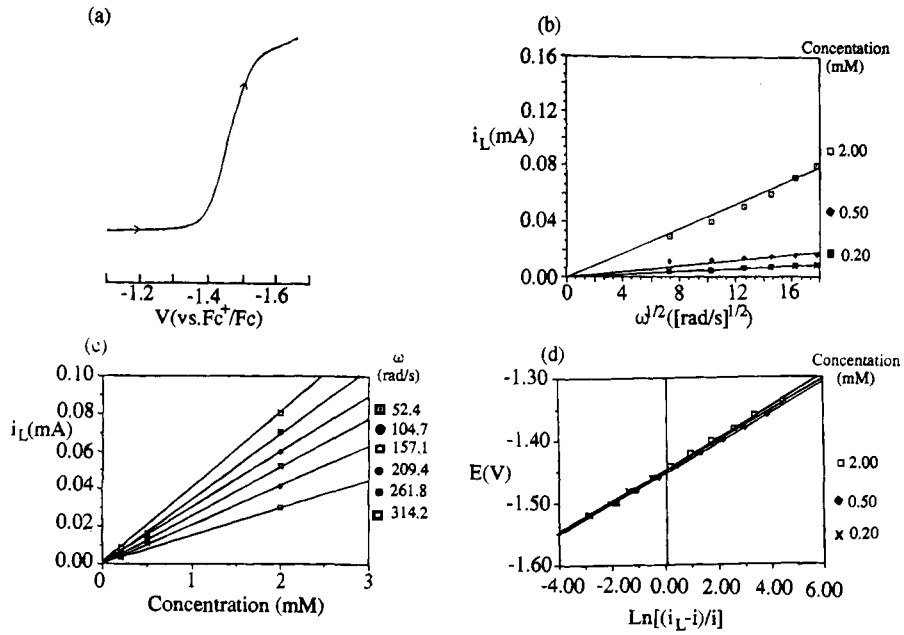

Figure 4. Hydrodynamic voltammetry (ν, 100 mV s^{-1}; 25 °C) at a rotating glassy-carbon disk electrode for $MoS_2(C_5H_{10}NO)_2$ solutions in DMF (0.2 M $Bu^n_4NBF_4$): (a) 2 mM, electrode rotation rate, ω = 157 rad s^{-1}; (b) concentration dependence of limiting current, i_L, on $\omega^{1/2}$; (c) dependence of i_L on concentration at different electrode rotation rates; (d) concentration dependence of plots of potential, E, versus $\ln[(i_L - i)/i]$; ω = 157 rad s^{-1}.

$$Mo^{VI}S_2(C_5H_{10}NO)_2 + e^- \leftrightarrow [Mo^{V}S_2(C_5H_{10}NO)_2]^- \quad (1)$$

The weak EPR signal (g 1.962) observed to be present during reductive electrolysis carried out in the cavity of an ESR spectrometer (Figure 2b) may be due to $[Mo^{V}S_2(C_5H_{10}NO)_2]^-$ since the signal disappeared immediately upon interruption of electrolysis.

$MoS_2(C_5H_{10}NO)_2$: The Chemical Step. Interaction of the reduced species $[MoS_2(C_5H_{10}NO)_2]^-$ with adventitious H_2O or O_2 might explain the exchange of sulfur with oxygen and the subsequent observation of the second and third reduction processes (Figure 1a). However, no significant variation in voltammetric behavior was observed in experiments in a closed cell in a glovebox under an argon atmosphere containing less than 1 ppm O_2 and H_2O indicating that the presence of these species does not contribute significantly to the oxygen exchange reactions. Similarly, deliberate addition of excess water did not affect the voltammetric data. Finally, voltammetric data also are inconsistent with the hypothesis that exchange occurs with O_2 or H_2O. If a reaction such as that of eq 2 occurred, then $[MoOS(C_5H_{10}NO)_2]^-$ would be generated at a potential at which oxidation reaction 3 would occur (Figure 1). With this

$$MoS_2(C_5H_{10}NO)_2 + e^- \leftrightarrow [MoS_2(C_5H_{10}NO)_2]^- + H_2O \rightarrow MoOS(C_5H_{10}NO)_2^- + H_2S \quad (2)$$

$$[MoOS(C_5H_{10}NO)_2]^- \leftrightarrow MoOS(C_5H_{10}NO)_2 + e^- \quad (3)$$

combination of a one-electron reduction process followed by a one-electron oxidation process, only small currents and n_{app} < 1 would be observed. Clearly, this is not the case, so

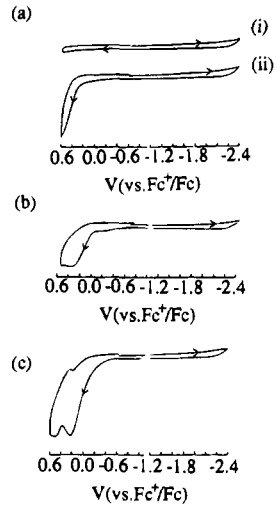

Figure 5. Cyclic voltammograms (v, 300 mV s^{-1}; 25 °C) at a glassy-carbon electrode for oxidation of various solutions in DMF (0.2 M $Bu^n_4NBF_4$): (a) (i) background; (ii) 2.0 mM $C_5H_{10}NH$; (b) 2.0 mM $C_5H_{10}NOH$; (c) mixture of 2.0 mM $C_5H_{10}NH$ and 2.0 mM $C_5H_{10}NOH$.

voltammetric evidence also appears to rule out reaction of $[MoS_2(C_5H_{10}NO)_2]^-$ with H_2O or O_2 as the origin of the interconversion.

In view of the above data, it appears likely that the chemical step following the initial one-electron reduction is a redox reaction involving the ligand $C_5H_{10}NO^-$. It may be relevant that both reduced ligand $C_5H_{10}NH$ and free ligand $C_5H_{10}NOH$ were observed by ^{13}C NMR as products in the cyanide-induced desulfurisation of $MoXY(C_5H_{10}NO)_2$ (XY = OS, SS).[14] In fact, oxidation processes characteristic of a mixture of $C_5H_{10}NOH$ and $C_5H_{10}NH$ are observed at positive potentials on the reverse scans in cyclic voltammograms after reduction of $MoS_2(C_5H_{10}NO)_2$ has occurred (Figure 1a). The peak for the oxidation of pure $C_5H_{10}NH$ occurs outside the DMF solvent limit but the onset of the response is readily detectable by comparison with the background voltammogram (Figure 5a). The voltammetric response for pure $C_5H_{10}NOH$ features two oxidation processes at −0.2 V and at about +0.6 V vs Fc^+/Fc (Figure 5b). When mixed, $C_5H_{10}NOH$ and $C_5H_{10}NH$ do not react, as determined by ^{13}C and ^1H NMR measurements. However, the voltammogram of a 1:1 mixture was not the sum of the individual responses (Figure 5c), suggesting that adsorption modifies the oxidation steps.

The response on the reverse scan of cyclic voltammograms implies that both the ligand, $C_5H_{10}NOH$, and reduced ligand $C_5H_{10}NH$ formed are generated upon reduction of $[MoS_2(C_5H_{10}NO)_2]$ (Figure 1a). This result is confirmed on the synthetic time scale by ^{13}C NMR identification[14] of these species produced in bulk electrolysis experiments. The presence of reduced ligand implies that oxygen has been abstracted from a reduced form of the ligand.

However, the overall process in which $MoOS(C_5H_{10}NO)_2$, $MoO_2(C_5H_{10}NO)_2$, $C_5H_{10}NOH$ and $C_5H_{10}NH$ are produced from $MoS_2(C_5H_{10}NO)_2$ must be complex as one mole of ligand $C_5H_{10}NO^-$ must be consumed for every sulfur atom that is exchanged for oxygen. The maximum yields of $MoOS(C_5H_{10}NO)_2$ and $MoO_2(C_5H_{10}NO)_2$ therefore cannot be greater than 67% and 50% respectively. The fate of both the thio ligands and the residual molybdenum is unknown, but they may contribute to the insoluble products formed on the electrode surface during bulk electrolysis. A similar stoichiometric uncertainty was characteristic of the cyanolysis reactions studied previously.[14]

$MoOS(C_5H_{10}NO)_2$. Cyclic voltammograms of *spectroscopically pure* $MoOS(C_5H_{10}NO)_2$ at room temperature are irreversible, and show the production of $MoO_2(C_5H_{10}NO)_2$ (Figure 1b) as well as reduced and free ligand. At lower temperatures, some degree of chemical reversibility is observed[13] indicating the transient existence of $[MoOS(C_5H_{10}NO)_2]^-$. No response attributable to $MoS_2(C_5H_{10}NO)_2$ was observed under any conditions indicating that the exchange reaction 4 does not occur on the voltammetric time scale.

$$2[Mo^VOS(C_5H_{10}NO)_2]^- \rightarrow [Mo^VS_2(C_5H_{10}NO)_2]^- + [Mo^VO_2(C_5H_{10}NO)_2]^- \quad (4)$$

The current function, $i^{red}_p v^{-1/2}$, is independent of concentration and is approximately 1.5 times that of $MoS_2(C_5H_{10}NO)_2$. Assuming that the diffusion coefficient of $MoS_2(C_5H_{10}NO)_2$ and $MoOS(C_5H_{10}NO)_2$ are similar, then this result suggests that $n_{app} > 1$ (n_{app} = apparent number of electrons associated with the charge transfer step) and that formation of an electrochemically reducible compound after the initial electron transfer process rather than a slow initial electron transfer step is responsible for the irreversible nature of the response. Overall, the reduction process for $MoOS(C_5H_{10}NO)_2$ has similar characteristics to that for reduction of $MoS_2(C_5H_{10}NO)_2$ and probably differs only in the sense that the chemical reactions occurring after the initial one electron charge transfer step are much faster.

A hydrodynamic voltammogram for reduction of $MoOS(C_5H_{10}NO)_2$ with a DC scan rate of 100 mV s^{-1} and an electrode rotation rate of 157 rad s^{-1} is shown in Figure 6a. Plots of i_L versus $\omega^{1/2}$ are close to linear and pass near the origin for each concentration examined (Figure 6b). Plots of i_L versus concentration are linear and pass through the origin at rotational frequencies above 157 rad s^{-1} (Figure 6c). Below this frequency, the plots are nonlinear indicating that the process is not strictly limited by diffusional mass transfer under all conditions and that the process is kinetically complicated. These data imply that the response at a rotating disk electrode is not simple. Importantly, i_L is, on average, 1.9 ± 0.2 times larger than for the corresponding experiments with $MoS_2(C_5H_{10}NO)_2$. The reduction process for $MoS_2(C_5H_{10}NO)_2$ was shown to be essentially a one-electron reversible charge transfer process on the hydrodynamic voltammetric time scale. Assuming that the diffusion coefficients for $MoS_2(C_5H_{10}NO)_2$ and $MoOS(C_5H_{10}NO)_2$ are similar, it follows that at ambient temperatures the limiting current for reduction of $MoOS(C_5H_{10}NO)_2$ is the result of an overall irreversible process involving the transfer of approximately two electrons.

Plots of E versus $\ln[i_L - i)/i]$ are given for different concentrations in Figure 6d. The $E_{1/2}$ value is −1.74 ± 0.01 V vs Fc^+/Fc but the slope is much greater than the 26 mV expected theoretically for a reversible one-electron charge transfer process and it is concentration dependent. These data also indicate that the rate of the chemical reaction accompanying the initial one electron transfer was too fast in the case of $MoOS(C_5H_{10}NO)_2$ to be eliminated by the use of hydrodynamic voltammetry and confirm the complexity of the overall process.

$MoO_2(C_5H_{10}NO)_2$. Cyclic voltammograms for the reduction of $MoO_2(C_5H_{10}NO)_2$ are chemically irreversible at all scan rates (10 to 1000 mV s^{-1})and temperatures (−60 to + 60 °C) examined. However, the free ligand and reduced form of the ligand are still observed on the reverse scan (Figure 1c) as is the case for reduction of $MoS_2(C_5H_{10}NO)_2$ and $MoOS(C_5H_{10}NO)_2$. The concentration dependence is difficult to study because of the close proximity of the compound reduction and solvent background processes. However, for a 2.00 mM solution, the current function $i^{red}_p v^{-1/2}$ decreases slightly with

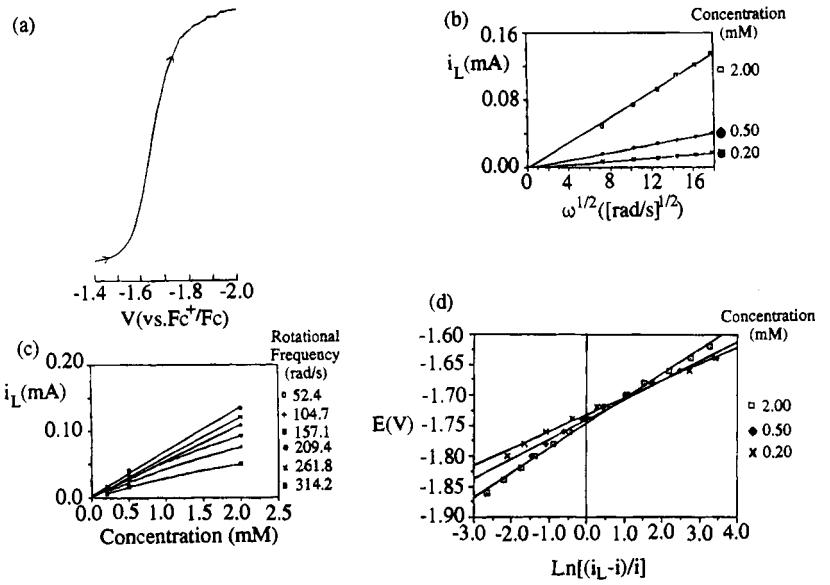

Figure 6. Hydrodynamic voltammetry (v, 100 mV s^{-1}; 25 °C) at a rotating glassy-carbon disk electrode of $MoOS(C_5H_{10}NO)_2$ solutions in DMF (0.2 M $Bu^n_4NBF_4$): (a) 2 mM; $\omega = 157$ rad s^{-1}; (b) concentration dependence of limiting current, i_L, on $\omega^{1/2}$; (c) dependence of i_L on concentration at different electrode rotation rates. (d) concentration dependence of potential, E, versus $\ln[(i_L - i)/i]$; $\omega = 157$ rad s^{-1}.

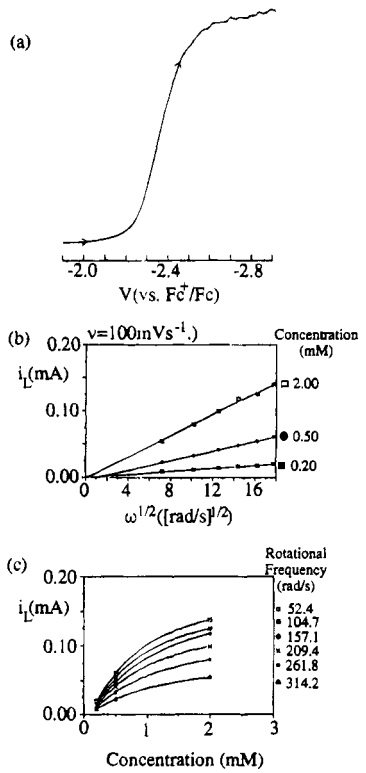

Figure 7. Hydrodynamic voltammetry (v, 100 mV s^{-1}; 25 °C) at a rotating glassy carbon disk electrode of $MoO_2(C_5H_{10}NO)_2$ solutions in DMF (0.2 M $Bu^n_4NBF_4$): (a) 2 mM, $\omega = 157$ rad s^{-1}; (b) concentration dependence of limiting current, i_L, on $\omega^{1/2}$; (c) dependence of i_L on concentration at different electrode rotation rates.

increasing v. On average, the value is 1.6 times larger than the current function for $MoS_2(C_5H_{10}NO)_2$, implying, as is the case with $MoOS(C_5H_{10}NO)_2$, that chemical steps and a second one-electron charge transfer step occur after formation of $[MoO_2(C_5H_{10}NO)_2]^-$.

Hydrodynamic voltammograms (Figure 7a) suggest that the reduction of $MoO_2(C_5H_{10}NO)_2$ is kinetically complex. Plots of i_L vs $\omega^{1/2}$ are linear, but do not pass through the origin (Figure 7b), while plots of i_L versus concentration are nonlinear at all rotation speeds examined (Figure 7c). Assuming equal diffusion coefficients for $MoO_2(C_5H_{10}NO)_2$ and $MoS_2(C_5H_{10}NO)_2$, then the value of n_{app} was found to lie in the range 2.4 ± 0.6 as determined from the ratio of i_L for reduction of $MoO_2(C_5H_{10}NO)_2$ and $MoS_2(C_5H_{10}NO)_2$ ($n = 1$) over the concentration range 0.5−2.0 mM. At the highest concentration of 2.0 mM, where problems with the background current correction were least, the value was 1.9 ± 0.1 and the most probable n value is therefore 2. The reduction of $MoO_2(C_5H_{10}NO)_2$ again presumably occurs via a complicated electron transfer, chemical reaction, electron transfer sequence of events. However, for the $MoO_2(C_5H_{10}NO)_2$ complex, the chemical step occurring after the initial charge transfer process appears to be even more rapid than is the case with reduction of $MoOS(C_5H_{10}NO)_2$, and no direct evidence was obtained for the existence of the one-electron reduced species $[MoO_2(C_5H_{10}NO)_2]^-$.

The Electrochemical Pathway. With the longer time domain experiments electrochemical reduction of the Mo^{VI}–thio species produces Mo^{VI}–oxo compounds in yields of less than 50%. The protonated form of the ligand, $C_5H_{10}NOH$, and the reduced form of the ligand, $C_5H_{10}NH$, also are observed as products. The overall reduction processes are irreversible and occur with approximately two electrons being transferred per molecule of compound being reduced. However, at short time scales or at low temperature, voltammetric reduction of these compounds approaches a reversible one-electron process to give $[MoS_2(C_5H_{10}NO)_2]^-$ and $[MoOS(C_5H_{10}NO)_2]^-$ as the only product.

The primary step in the reduction process is reasonably represented for all compounds as the metal-based reduction of $Mo^{VI}X_2(C_5H_{10}NO)_2$ to $[Mo^{V}X_2(C_5H_{10}NO)_2]^-$. The uptake of a second reducing equivalent may cause the overall irreversibility observed in the longer time domain experiments. Cyclic and rotating disk voltammetric data are consistent with a complex form of a process involving an electron transfer, chemical reaction, and electron transfer type sequence of events.

Production of the oxo-substituted species from reduced $[Mo^{V}S_2(C_5H_{10}NO)_2]^-$ appears to be associated with oxygen transfer from the ligand, with reduction of the ligand being achieved by an internal redox reaction followed by uptake of the second electron. A complex series of reactions follow which generate the final reaction products which include $MoOS(C_5H_{10}NO)_2$, $MoO_2(C_5H_{10}NO)_2$, $C_5H_{10}NOH$, $C_5H_{10}NH$, and other unidentified products. Free protonated ligand $C_5H_{10}NOH$ cannot

be reduced in the available potential range, but ligation to Mo^V apparently induces an internal redox process.

Remarkably, the net result of the reductive electrochemistry and cyanolysis reactions[14] are very similar. The clearest comparison is for the dithio species where the cyanolysis reaction can be represented by eq 5. In this reaction, cyanide

$$Mo^{VI}S_2(C_5H_{10}NO)_2 + 2C_5H_{10}NO^- + 2H^+ + 2CN^- \rightarrow Mo^{VI}O_2(C_5H_{10}NO)_2 + 2C_5H_{10}NH + 2SCN^- \quad (5)$$

appears to act as both the source of initial reducing equivalents and the trap for oxidized sulfur. However, the identity of the sulfur product in the reductive electrochemistry is unknown, but it is certainly not soluble elemental sulfur. Insoluble products are adsorbed or precipitated onto an electrode surface after the two-electron irreversible reaction and may be responsible for the lack of observation of sulfur byproducts and also account for the deficiency in molybdenum. For example, the formation of various polyoxothiomolybdates is possible. These species are generally insoluble and would not be observed electrochemically or by NMR.

As the reduction potential becomes more negative, the ligand-based reaction becomes progressively more rapid and the detection of Mo^V intermediates more difficult. Thus, $MoO_2(C_5H_{10}NO)_2$, which is reduced at very negative potentials, displays totally irreversible behavior and the postulated $[MoO_2(C_5H_{10}NO)_2]^-$ intermediate is not observed under the conditions examined. However, in the case of $MoOS(C_5H_{10}NO)_2$, which is reduced at intermediate potentials, $[MoOS(C_5H_{10}NO)_2]^-$ is observable at short time domains with the n_{app} value being intermediate between 1 and 2 depending on the conditions. Finally, the most easily reduced $MoS_2(C_5H_{10}NO)_2$ leads to ready observation of $[MoS_2(C_5H_{10}NO)_2]^-$.

Scheme 1

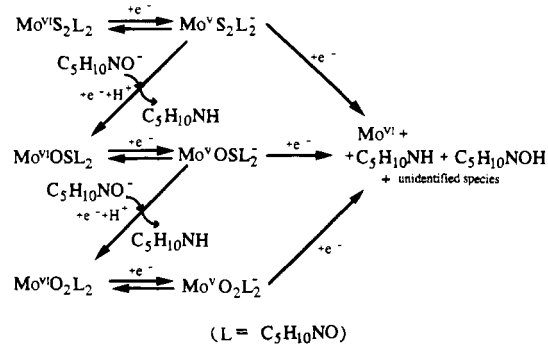

While a definitive account of the complete mechanism cannot be deduced from the present studies, the reaction scheme shown in Scheme 1 represents a summary of some of the features which have been identified.